International Journal of Nanoelectronics and Materials
Volume 13, No. 3, July 2020 [433-444]

Structural and Morphological Properties of $Cu_{1-x}Al_xO$ Nanostructures Prepared by sol-gel Method

Ziad T. Khodiar[1], Nadir F. Habubi[2]*, Intessar K. Abd[1], and Ahmed M. Shano[3]

[1]*University of Diyala, College of Education of Pure Science, Diyala, Iraq.*
Mustansiriyah University, College of Education, Baghdad, Iraq.
[3]*Bilad Alrafidain University College, Department of radiological techniques, Diyala, Iraq.*

Received 21 August 2019, Revised 25 March 2020, Accepted 11 May 2020

ABSTRACT

In this study, the sol-gel process has been adopted for the synthesis of $Cu_{1-x}Al_xO$ nanostructures ($0 \leq x \leq 0.90$, in steps of 0.10). The system revealed pure CuO phase with monoclinic structure. Al_2O_3 phase and copper oxide (Cu_2O) were developed at higher substituent concentrations till x=0.40. Structural properties were studied by X-ray diffraction (XRD) and morphological properties by Scanning Electron Microscope (SEM). Average crystallite size from the range of 12.65 nm to 22.9 nm was calculated by Scherer formula. The SEM images indicated that the $Cu_{1-x}Al_xO$ possessed nanoparticles like structure, i.e. it contained some pores or voids and vacancies caused by a difference in experimental conditions. Results of EDX revealed the presence of Aluminum (Al), oxygen (O) and copper (Cu) elements in $Cu_{1-x}Al_xO$ and the data showed that the nanoparticles were nearly stoichiometric.

Keywords: $Cu_{1-x}Al_xO$, Sol-gel method, Structural Properties.

1. INTRODUCTION

In chemical sciences, synthesis of transition metal and metal oxide nanoparticles is a growing research priority. Metal oxide nanoparticles is a highly valuable material with various applications in optical, electrical and mechanical devices, catalysts, gas sensors and sunscreens [1]. As the metal particles are reduced in size, bulk properties of the particles disappear to be substituted to that of quantum dot following quantum mechanical rules. It can thus be easily understood that metal nanoparticles chemistry differs from that of the bulk materials because of size reduction, the high surface area to volume ratio enhances the catalytic activity [2]. Among various metal nanoparticles, copper (Cu) and copper oxide (Cu_2O) nanoparticles have attracted considerable attention because copper is one of the essential materials in modern technologies and is readily available [3]. In recent years, copper(ll)-oxide nanoparticles (CuO-NPs), which belong to the monoclinic structure system, have attracted growing interest for both fundamental and practical reasons. They have different wide applications based on the physical and chemical properties, such as superconductivity, photovoltaic properties, relatively stable, low cost and antimicrobial activity [4]. Nowadays, the applications of CuO-NPs are crucial to antioxidants [5], antibacterial, thermal conductivity, catalytic, battery [6, 7] and solar cells [8]. Transition metal oxides are the important class of

*Corresponding Author: *nadirfadhil@uomustansiriyah.edu.iq*

semiconductors, which have applications in magnetic storage media and electronics. Among transition metal oxides, copper oxide nanoparticles are of special interest because of their greater efficiency as nanofluids in heat transfer applications. For example, it has been reported that 4% addition of CuO improves the thermal conductivity of water by 20% [9]. Nanostructured materials have been prepared with different sizes and shapes ranging from thermal reduction, sonochemical method, co-precipitation, sol-gel method, and so forth [10-12]. The aim of the present study is to synthesis $Cu_{1-x}Al_xO$ using the sol-gel method from copper and aluminium saults and examine their structural and morphological properties.

2. EXPERIMENTAL DETAILS

Sol-gel method was used for the synthesis of $Cu_{1-x}Al_xO$ at x = 0, 0.10, 0.20, 0.30, 0.40 and 0.50 using high-purity materials: (i) Copper nitrate $Cu(NO_3)_2.3H_2O$ (99.0%), and (ii) Aluminum nitrate nonahydrate $Al(NO_3)_3.9H_2O$ (99%). The mixture of metals nitrates was dissolved in 200 mL of distilled water with 1:1 M ratios to form aqueous solutions with continuous magnetic stirring at room temperature for 30 minutes on a hot-plate magnetic stirrer. When the solution blended and the dissolution for the raw materials completed, the liquid ammonia was slowly added to neutralize solution until pH=7 with continuous stirring. The temperature of hot plat-stirrer was gradually increased to reach (80ºC) with continuous stirring and was kept on heating at this temperature, then the water evaporated from the solution and the sol gradually changed into a gel. Afterwards, the formed viscous gel was put in the oven to dry at 110ºC for one hour. The dry gel was annealed at 300ºC for 1 hour in the air to remove the impurities and nitrates. The powder was cooled down in the furnace so that the cations could fit at their equilibrium positions. Later, an amount of powder was removed to be measured for its structural properties.

3. RESULTS AND DISCUSSIONS

3.1. X-ray Diffraction (XRD) Results

The X-ray diffraction (XRD) patterns of $Cu_{1-x}Al_xO$ samples (x = 0, 0.10, 0.20, 0.30, 0.40 and 0.50) for phase identification performed by the XRD are shown in Figure 1. The presence of the diffraction peaks corresponding to the planes (110), $(11\bar{1})$, (111), $(20\bar{2})$, (020), (202), $(11\bar{3})$, (310), (220), $(31\bar{1})$, (113) and $(22\bar{2})$ indicates that the studied samples have CuO monoclinic structure according to the standard ICDD card no.(00-048-1548). The indexed diffraction peaks were used to calculate the interplanar spacings (d_{hkl}) corresponding to the (110), $(11\bar{1})$, (111), $(20\bar{2})$, (020), (202), $(11\bar{3})$, (310), (220), $(31\bar{1})$, (113) and $(22\bar{2})$ planes indicate that the studied CuO samples are polycrystalline, monoclinic structure according to the standard ICDD card no.(00-048-1548) with the best-preferred orientation $(11\bar{1})$, (111), $(20\bar{2})$ [6] as shown in Table (1). The main diffraction peaks in all XRD patterns match with those for the standard pattern of CuO and are following those of the previous study [13]. The small shift of the diffraction peaks toward smaller angular positions for the sample with x=0.10 compared to sample with x=0 may be due to the interstitial of Al^{+3} ions into the CuO lattice, which leads to increase the interplanar spacings (d_{hkl}) because the ionic radius of

Al^{+3} and Cu^{+2} is 0.53Å and 0.73Å, respectively [14]. The small shift this peak 0.30 compared with x=0.10, this behaviour indicates a decrease in interplanar spacings of CuO lattice due to the substitution of Al^{+3} ions into the Cu^{+2} sites, but the full width at half maximum (FWHM) mostly which respond to the decrease or increase in crystallites size, where it is increased at x=0.50 compared with x=0 [10, 14]. There is an increase in interplanar spacings for x=0.40 and x=0.50 compared with x=0, therefore, beyond x= 0.40, a saturation of substitutional sites takes place and this leads to another mode of Al incorporation, which seems to privilege the interstitial sites and might lead to an amorphization. However, according to the relative values of diffraction intensities, the excessive addition of aluminium (x=0.50) leads to the crystallite disorientation, which tends to an amorphization of material and decreased in crystallinity with increasing Al^{+3} substitution. Therefore, the analysis of this phenomenon is that the excessive introduction of aluminium into the interstitial sites will generate a great number of defects from the distortion of the crystal structure of material [15]. Extra diffraction peaks at 43.28° and 50.41° were also observed in the samples with x=0.40($Cu_{0.6}Al_{0.4}O$) which indicates the presence of a small amount of Al_2O_3 phase in these samples with pdf card no. 090440. Therefore, it can be concluded that Al ions with concentrations in the range reported in this study substitute Cu ions in the $Cu_{0.6}Al_{0.4}O$ lattice without affecting its monoclinic structure. The peaks at 2θ = 36.39°, 42.26 and 29.53 are related to the Cu_2O phase with ICDD card no. (00-005-0667). This peak appeared because they require calcination above 300°C to fully oxygenated of the CuO compound. At x=0.50, the intensities and the number of peaks decreased due to the decreased in crystallinity with increasing Al^{+3} substitution.

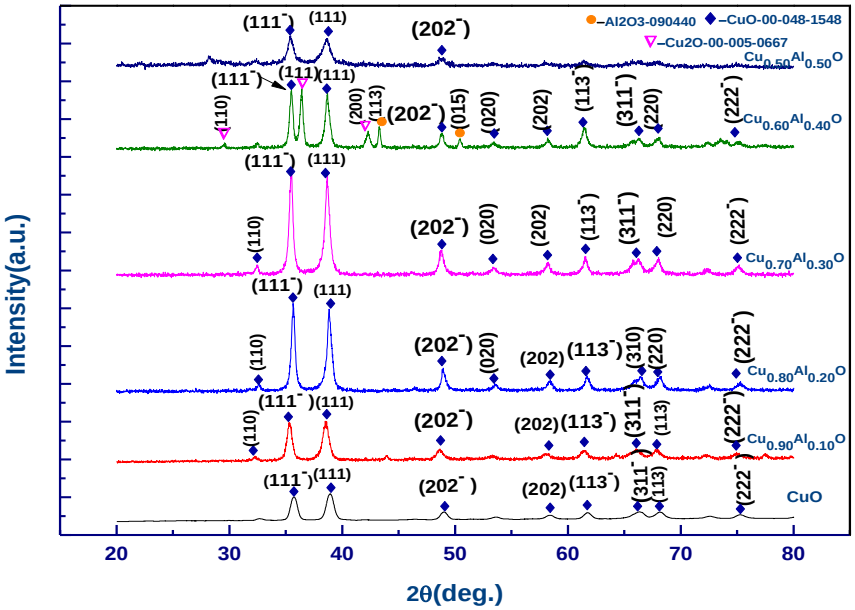

Figure 1. XRD patterns of the $Cu_{1-x}Al_xO$ at (x=0, 0.10, 0.20, 0.30, 0.40 and 0.50).

Table 1 Result of XRD of the strongest three peaks for $Cu_{1-x}Al_xO$ where (x=0, 0.10, 0.20, 0.30, 0.40 and 0.50)

Sample	2θ (deg)	d_{hkl} (Å)	*hkl*	FWHM (deg)
X=0	35.7235	2.5114	$(11\bar{1})$	0.4674

	38.9214	2.3121	(111)	0.5437
	48.9904	1.8579	$(20\bar{2})$	0.49
X=10	35.3380	2.53791	$(11\bar{1})$	0.5733
	38.5495	2.33355	(111)	0.6807
	48.6289	1.87082	$(20\bar{2})$	0.6666
X=20	35.6566	2.51596	$(11\bar{1})$	0.3835
	38.8743	2.31479	(111)	0.4636
	48.9507	1.85927	$(20\bar{2})$	0.3840
X=30	35.4690	2.52884	$(11\bar{1})$	0.409
	38.6732	2.32637	(111)	0.481
	48.7688	1.86578	$(20\bar{2})$	0.483
X= 40	35.4898	2.52740	$(11\bar{1})$	0.3516
	36.3961	2.46652	(111)	0.3314
	38.6889	2.32546	(111)	0.4244
X=50	35.4284	2.53164	$(11\bar{1})$	0.6182
	38.5915	2.33110	(111)	0.8267
	48.7698	1.86575	$(20\bar{2})$	0.6980

Table 2 shows the results of the lattice parameters 'a', 'b' and 'c', c/a, a/b and c/b ratios, cell volume, x-ray density and average crystallite size for $Cu_{1-x}Al_xO$. The lattice parameters (a, b and c) were calculated from the XRD data using the following equation [16]:

$$\frac{1}{d^2} = \left[\frac{\frac{h^2}{a^2} + \frac{l^2}{c^2} - \frac{2hl\cos\beta}{ac}}{\sin\beta^2} + \frac{k^2}{b^2} \right] \quad (1)$$

From Table 2, it is clear that the values of the lattice constants for CuO are in agreement with the values of the (ICDD) standard cards for CuO (a_o=4.688Å, b_o=3.422Åand c_o=5.131 Å) and with those of the previous study [17]. There are various causes of the variation of the lattice parameters such as variation of stresses within the phases, temperature variation, changes in the chemical composition of the phases. It can be observed that the values of the lattice constants of the prepared oxide with different mixing ratios are shifted from their values of CuO oxide and hose in the (ICDD) standard cards. This deviation is due to the replacement of the two compounds ions with each other since the diameter of copper ions is (0.73 Å), which is greater than the diameter of aluminium ions (0.53 Å) [12].

Cell volume is calculated from the following equation [18]:

$$V = abc\ sin\beta \quad (2)$$

Where β is 99.54 for the monoclinic structure. These values are consistent with the reported values in the literature [18].

X-ray density is calculated from the following equation [18]:

$$D_x = \frac{4M}{N_A V} \quad (3)$$

Where M is the molecular mass of CuO, N_A is the Avogadro number and V is the volume of the unit cell. This variation in X-ray density for CuO monoclinic oxide with different concentrations was due to the variation in unit cell volume as X-ray density is inversely proportional to the cell volume which increased with decreasing cell volume and decreased as it increased. Furthermore, the variation was also due to the presence of phase impurity in a lattice and the substitution of Al ions in Cu ions. These values are consistent with the reported values in the literature [18].

Average crystallite size is determined from the position of the three strongest peaks using Scherer's formula [17, 19] as shown in the following equation.

$$D = \frac{K\lambda}{\beta \cos\theta} \quad (4)$$

Where D is the mean size of crystallites (nm), 'K' is crystallite shape factor, a good approximation is 0.9, λ is x-ray wavelength 1.5406 Å, 'β' is the line broadening in the middle of the maximum intensity (FWHM) and θ is the Bragg angle. Table (2) shows that the average crystallite size in the range (12.65 - 22.9) is in accordance with reported values [17]. The values change unsystematically, increased one time and decreased the other. This behaviour is because of the phase changes or the Al ions substituted Cu ions. The broadening of the diffraction peaks indicates that the crystal size is small. In the case of pure CuO spectrum, the diffraction peaks are considerably broadened and caused by the small crystallite sizes. Small crystallites have relatively few lattice planes that contribute to the diffraction lines. Broadening the peak may also occur due to micro straining of the crystal structure arising from defects such as its location and twinning.
The density of dislocation (δ) is determined by [20].

$$\delta = \frac{1}{D_{av}^2} \quad (5)$$

Table 2 shows that the average crystallite size for all samples in the range (16.2-10.64 nm) calculated for (111) direction. The estimated crystallite sizes are listed in Table (2). A change in the lattice parameter is observed for Al-doping. The grain sizes are changed unsystematically depending on both crystallographic axes and doping concentrations as shown in Figure 2. When Al atoms are doped in the CuO nanoparticles, they replace the crystal lattice of Cu. Since the atomic radii of Cu and Al are different [14], some Al atoms prefer to locate in/near the grain boundary regions, which might prevent grain growth. Therefore, the grain size decreases as the concentration of Al concentration doped in the nanoparticles increases, which are good agreement with the result when x=0.0, 0.10 and 0.50. Whereas at concentrations 0.20, 0.30 and 0.40, there is a different behaviour and this may be due to the doping, which is considered as the main factor that would cause the lattice distortion (a, b and c) of the crystals, for it is usually different from the atomic radii of different elements, and discussed in details as Cu can exist in Cu^{+}, Cu^{2+} and Cu^{3+} ions having ionic radii 0.77 Å, 0.73 Å and 0.54 Å, respectively. In this study, the stress of synthesizing A-doped Cu nanoparticles is tensile stress. The crystallite quality

0.20, 0.30 and 0.40 of Al is different than the crystallite quality of the undoped CuO nanoparticles [21- 23].

The different volumes (V) of the unit cell shown in Table 2 show a slight decrease or increase, attributed to the defect or vacancies formation in the transition phase of Cu^{+}, Cu^{2+} and Cu^{3+} ions during the diffusion process. The value of X-ray density (D_x) shows a slight difference depends on the molecular weight of the sample as well as the volume of the unit cell [23].

The values of dislocation density (δ) of undoped and Al-doped CuO samples display a small variation value, this indicates the occurrence of crystal reorientation effect due to the change of the Al-dopants concentration [24].

Table 2 The XRD parameters of $Cu_{1-x}Al_xO$ where (x= 0, 0.10, 0.20, 0.30, 0.40 and 0.50)

Parameters	X=0	x=0.10	x=0.20	x=0.30	x=0.40	x=0.50
a (Å)	4.6957	4.686	4.710	4.692	4.679	4.697
b (Å)	3.4412	3.422	3.434	3.426	3.422	3.468
c (Å)	5.1349	5.120	5.118	5.120	5.131	5.126
c/a	1.093	1.092	1.086	1.091	1.096	1.091
a/b	1.364	1.369	1.371	1.369	1.367	1.354
c/b	1.492	1.496	1.490	1.494	1.499	1.478
V (Å^3)	81.822	81.090	81.760	81.289	81.143	82.470
D_x (g/cm^3)	6.443	6.517	6.464	6.501	6.513	6.408
D_{ave} (nm)	16.2	12.9	18.9	18.3	20.7	10.64
δ(line. cm^{-2})	0.0038	0.006	0.0027	0.0029	0.0023	0.0088

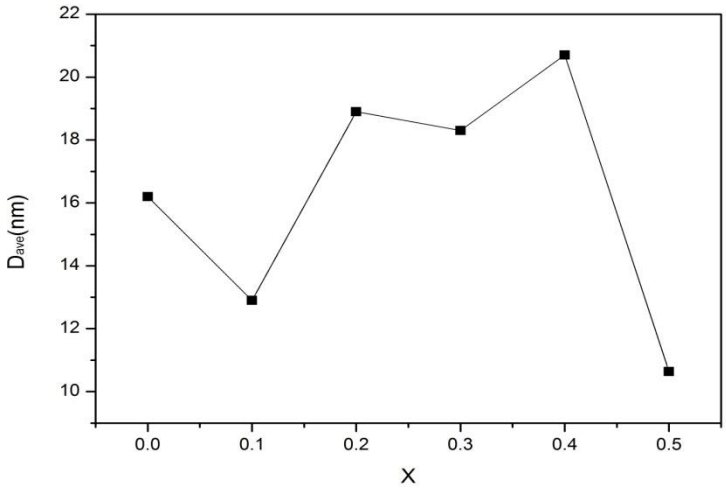

Figure 2. D_{ave}(nm) against X of $Cu_{1-x}Al_xO$ where (x=0, 0.10, 0.20, 0.30, 0.40 and 0.50).

3.2. Scanning Electron Microscopic (SEM) Analysis

Figure 3(a-f) is Scanning Electron Microscopic (SEM) images of $Cu_{1-x}Al_xO$. The SEM image at 50.00 kx magnifications was collected. From the SEM image of $Cu_{1-x}Al_xO$, it was observed that the particles were well-dispersed spherical accompanying almost well-defined and uniform crystalline structure. There was also a higher tendency of

agglomerations. The island growth of the tightly packed spherical arrangement was observed. In some regions, the big nanoparticles were surrounded by smaller nanoparticles. The SEM micrographs of the $Cu_{1-x}Al_xO$ that contain some pores or voids and vacancies were caused by the difference in experimental conditions, mainly the homogeneity of the material, which is in agreement with other reports [25]. In some places, various sizes of the particles (small and large size) are observed, i.e. packed spherical seem to be randomly distributed in the sample [25]. The SEM images of CuO-NPs is in agreement with the result obtained by Palaniradja *et al.* [26].

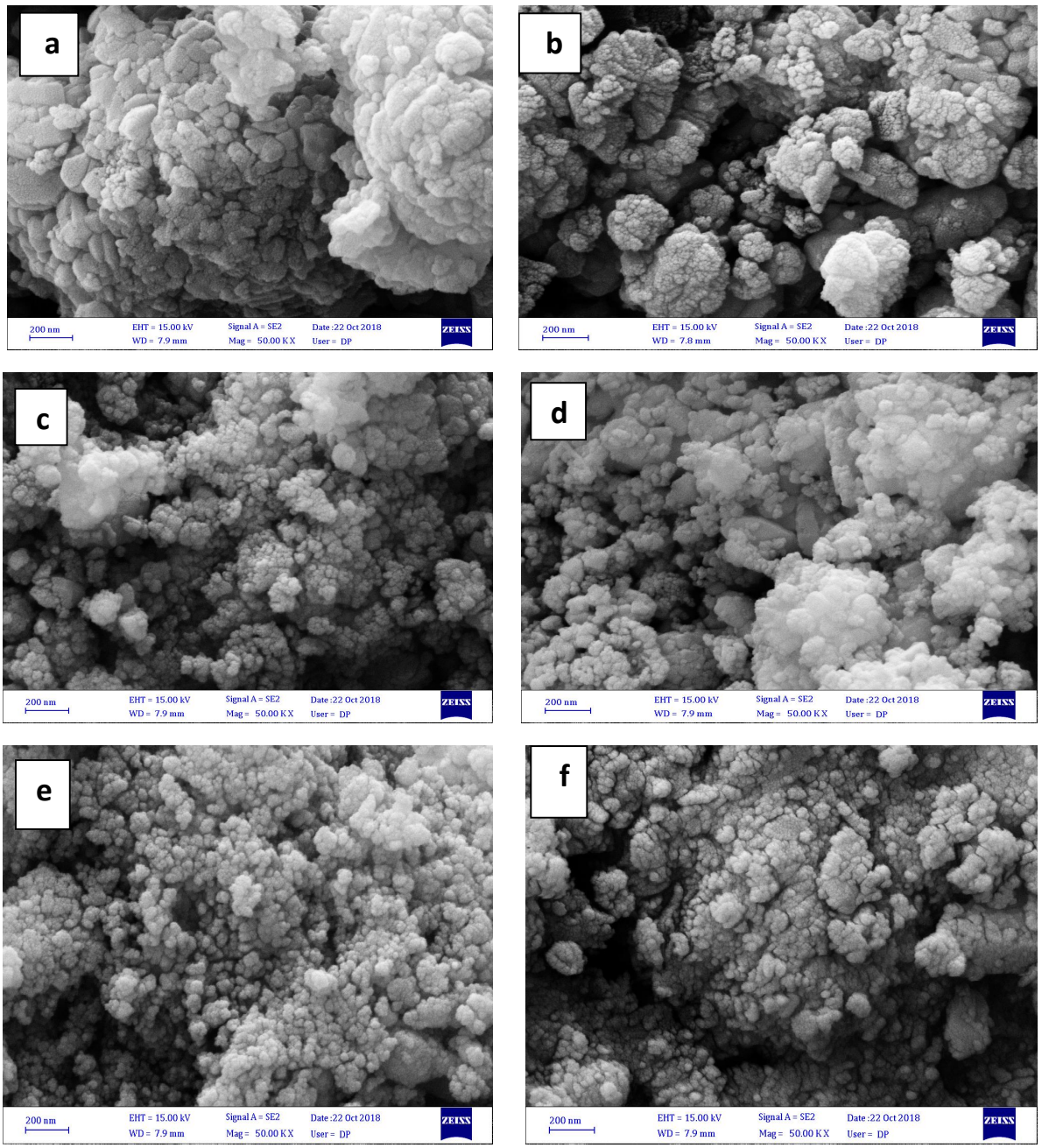

Figure 3(a-f). SEM image of $Cu_{1-x}Al_xO$ where (x=0, 0.10, 0.20, 0.30, 0.40 and 0.50).

3.3 Energy Dispersive X-ray (EDX) Analysis

Figure 4 shows the Energy Dispersive X-ray (EDX) analysis of $Cu_{1-x}Al_xO$. The Cu and Al peaks depict the characteristic chemical composition of the synthesized nanoparticles. The EDX analysis carried out $Cu_{1-x}Al_xO$ at 10 keV. Results revealed the presence of Aluminum (Al), oxygen (O) and copper (Cu) elements in $Cu_{1-x}Al_xO$. gold (Au) impurities are shown in the EDX spectra. It is noticed that the dominant composition is CuO whereas the quantitative analysis of the $Cu_{1-x}Al_xO$ shows a strong peak corresponding to Cu, which confirms the high purity of this comparison for $Cu_{1-x}Al_xO$. This confirms the entry of Al impurity within the crystal structure of CuO. The elemental analysis of the sample shows that the prepared sample is copper oxide, which is in good concord with the results of XRD. Similar results were reported elsewhere [26].

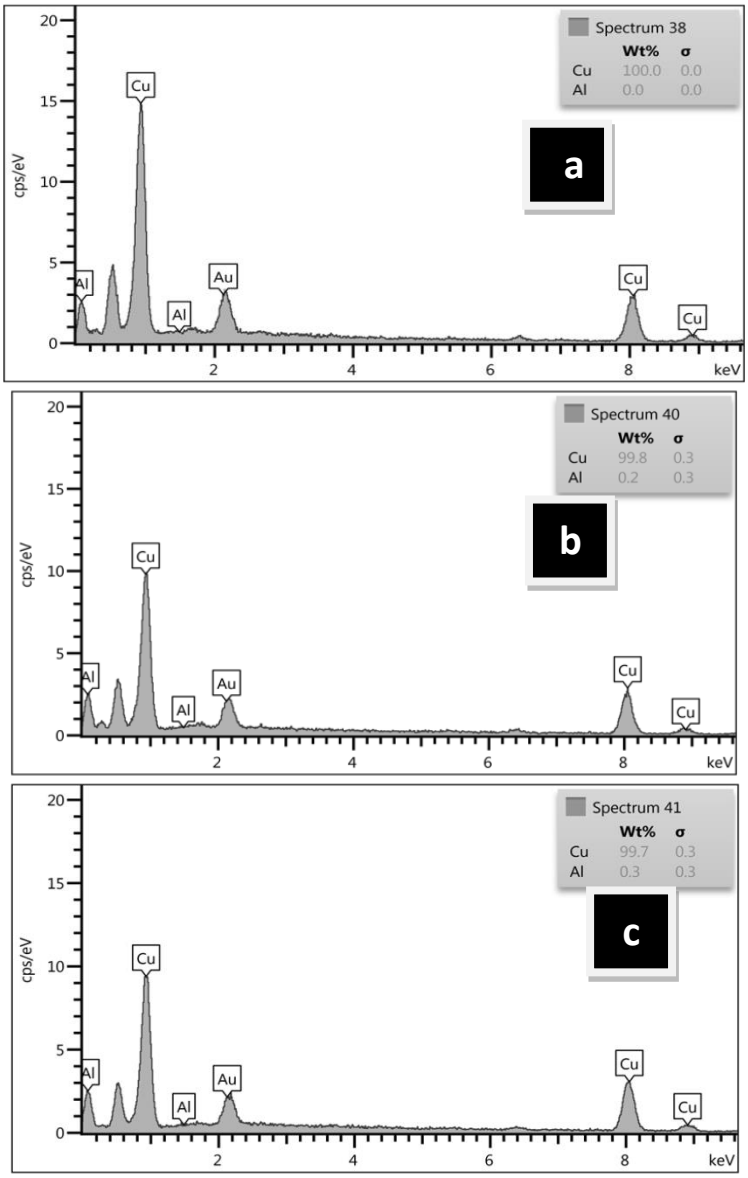

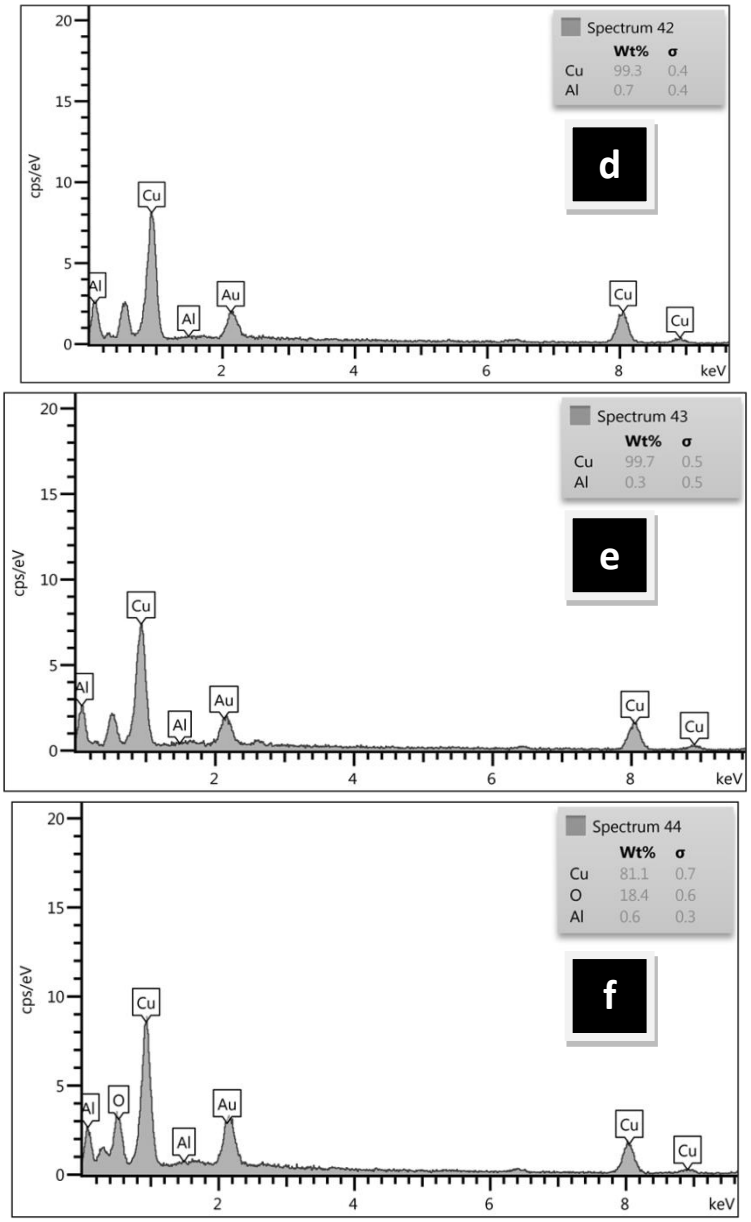

Figure 4. (a-f). Energy dispersive X-ray analysis of $Cu_{1-x}Al_xO$ where (x=0, 0.10, 0.20, 0.30, 0.40 and 0.50).

4. CONCLUSIONS

The sol-gel method has been adopted to synthesize $Cu_{1-x}Al_xO$ (x= 0, 0.10, 0.20, 0.30, 0.40, and 0.50). XRD analysis indicated that the samples showed pure CuO with monoclinic structure, which points to the fact that aluminium ions diffused completely into the copper monoclinic structure at low substitution. At higher substitution levels, however, the signature of the $Al_2O_3$and Cu_2O was observed. Average crystallite size changes unsystematically: decreased one time and increased the other as the ratio of aluminium oxide increases. The SEM images indicated that the $Cu_{1-x}Al_xO$ structure-like nanoparticles. Results of EDX revealed the presence of Aluminum (Al), oxygen (O) and copper (Cu) elements in $Cu_{1-x}Al_xO$.

REFERENCES

[1] Karim Henikish Hassan, Areej Ali Jarullah, Sally KamilSaadi, "Green synthesis and structural characterization of CuO nanoparticles prepared by using fig leaves extract" J. Pak. j. sci. ind. res. Ser. A: Phys. sci. **61**, 2 (2018) 59-65.

[2] M. S. Niasari, F. Davar & N. Mir, "Synthesis and characterization of metallic copper nanoparticles via thermal decomposition", Polyhedron **27** (2008) 3514-3518.

[3] M. J. G. Pacheo, J. E Morales-Sanchz, J. Gernandez and F. Ruiz, "Synthesis of copper nanoparticles using soybeans as a chelant agent", Material Letters **64** (2010) 1361-1364.

[4] V. Rai, B. Jamuna, Science Against Microbial Pathogens: "Communicating Current Research and Technological Advances", Mendez-Vilas., A.(Ed.). University of Mysore, India **197**(2011).

[5] Das, Dhaneswar, *et al.* "Synthesis and evaluation of antioxidant and antibacterial behavior of CuO nanoparticles." Colloids and Surfaces B: Biointerfaces **101** (2013) 430-433.

[6] Ziad T. Khodair, Ali M. Mohammad, Anees A. Khadom. "Investigations of structural and magnetic properties of $Cu_{1-x}V_xO$ nanostructures prepared by sol-gel method". Chemical Data Collections **25** (2020) 100315.

[7] Chandrasekaran, S. "A novel single step synthesis, high efficiency and cost effective photovoltaic applications of oxidized copper nanoparticles." Solar Energy Materials and Solar Cells **109** (2013) 220-226.

[8] Ziad T. Khodair, Mohanad W. Mahdi Alzubaidy, Asmaa M. Salih Almohaidi, Ammar Ahmed Sultan, Sana MH AL-Shimmary, Sarah S. Albusultan, " Synthesis of Copper Oxide Nanoparticles (CuO-NPs) and its Evaluation of Antibacterial Activity Against P. aeruginosa Biofilm Gene's" Technologies and Materials for Renewable Energy, Environment and Sustainability AIP Conf. Proc. 2190, 020006-1–020006-7 (2019).

[9] S. G. RejithandC. Krishnan, Synthesis of cadmium-doped copper oxide nanoparticles: Optical and structural characterizations, Advances in Applied Science Research **4**, 2 (2013) 103-109.

[10] Ahmed H. Abed, Tagreed M. Al- Saadi & Ziad T. Khodair. "Structural, electrical and magnetic properties of the ($Ce_xFe_{0.05}Mg_{0.95-x}O$) nano compound synthesized via sol-gel/ auto combustion technique" ARPN Journal of Engineering and Applied Sciences **13**, 19 (2018).

[11] Z. T. Khodair, N. A. Bakr, A. M. Hassan, A. A. Kamil. "Influence of substrate temperature and thickness on structural and optical properties of CZTS nanostructures thin films" Journal of Ovonic Research **15**, 6 (2019) 377- 385.

[12] A. M. Saleh, N. A. Bakr, Z. T. Khodair. "Effect of Oxygen Flow Rate On Structural and Optical Properties of SnO_2 Thin Films Prepared by APCVD Technique", Digest Journal of Nanomaterials and Biostructures **13**, 3 (2018) 603- 608.

[13] Mohammed Suleiman, Muath Mousa, Amjad Hussein, Belkheir Hammouti, Taibi B. Hadda, Ismail Warad. "Copper(II)-Oxide Nanostructures: Synthesis, Characterizations and their Applications–Review", J. Mater. Environ. Sci. **4**, 5 (2013) 792-797.

[14] Shannon, Robert D. "Revised effective ionic radii and systematic studies of interatomic distances in halides and chalcogenides". Acta crystallographica section A: crystal physics, diffraction, theoretical and general crystallography **32**, 5 (1976) 751-767.

[15] A. Nakrela, N. Benramdane, A. Bouzidi, Z. Kebbab, M. Medles, C. Mathieu, "Site location of Al-dopant in ZnO lattice by exploiting the structural and optical characterisation of ZnO:Al thin films". Results in Physics **6** (2016) 133-138.

[16] J. Connolly, "Elementary Crystallography for X-Ray Diffraction", Introduction to X-Ray powder diffraction, Spring, (2012).

[17] Jagdeep M. Kshirsagar, Ramakant Shrivastava, & Prakash S. Adwani, "Preparation and characterization of copper cxide nanoparticles and determination of enhancement in critical heat flux", Thermal science **21**, 1A (2017) 233-242.

[18] Thi Ha Tran & Viet Tuyen Nguyen, “Copper Oxide Nanomaterials Prepared by Solution Methods, Some Properties, and Potential Applications: A Brief Review”, Hindawi Publishing Corporation International Scholarly Research Notices, (2014) 14.

[19] Ziad T. Khodair, Buthainah Abdulmunem Ibrahim, Mayada Kaream Hassan," Investigation on the structural and optical properties of copper doped NiO nanostructures thin films" Materials Today: Proceedings 20 (2020) 560–565.

[20] Ziad T. Khodair, A. A. Kamil & Y. K. Abdalaah, "Effect of annealing on structural and optical properties of $Ni_{(1-x)}Mn_xO$ nanostructures thin films", Physica B**503**, 55-63 (2016).

[21] Shih-Shou Lo, Dison Huang, Chun Hsiang Tu, Chia-Hung Hou &Chii-Chang Chen, "Raman scattering and band-gap variations of Al-doped ZnO nanoparticles synthesized by a chemical colloid process". J. Phys. D: Appl. Phys. **42**, 095420 (2009) 5.

[22] M. K. R. Khan, M. Azizar Rahmana, M. Shahjahan, M. Mozibur Rahman, M. A. Hakim, Dilip Kumar Sahac, Jasim Uddin Khan, "Effect of Al-doping on optical and electrical properties of spray pyrolytic nano-crystalline CdO thin films". Current Applied Physics **10** (2010) 790-796.

[23] P. K. Labhane1, V. R. Huse1, L. B. Patle1, A. L. Chaudhari1, G. H. Sonawane, "Synthesis of Cu Doped ZnO Nanoparticles: Crystallographic, Optical, FTIR, Morphological and Photocatalytic Study". Journal of Materials Science and Chemical Engineering **3** (2015) 39-51.

[24] C. Aydın, H. M. El-Nasser, F. Yakuphanoglu, I. S. Yahia, M. Aksoy, "Nanopowder synthesis of aluminum doped cadmium oxide via sol–gel calcination processing" Journal of Alloys and Compounds **509** (2011) 854-858.

[25] Radhakrishnan, A. A. & Beena, B. B. “Structural and optical absorption analysis of CuO nanoparticles”. IndianJournal of Advances in Chemical Science **2** (2014) 158-161.

[26] Manimaran, R., Palaniradja, K., Alagumurthi, N., Sendhilnathan, S. & Hussain, J. “Preparation and characterization of copper oxide nanofluid for heat transfer applications”. Applied Nanoscience **4** (2014) 163-167.